Featured in Physics

Ultrastable Free-Space Laser Links for a Global Network of Optical Atomic Clocks

D. R. Gozzard,[1,2,*] L. A. Howard,[1] B. P. Dix-Matthews,[1,2] S. F. E. Karpathakis,[1]
C. T. Gravestock,[1] and S. W. Schediwy[1,2]

[1]*International Centre for Radio Astronomy Research, ICRAR M468, The University of Western Australia, 35 Stirling Hwy, Crawley 6009, Australia*

[2]*Australian Research Council Centre of Excellence for Engineered Quantum Systems, Department of Physics, School of Physics, Mathematics & Computing, The University of Western Australia, 35 Stirling Hwy, Crawley 6009, Australia*

(Received 24 June 2021; accepted 2 December 2021; published 14 January 2022)

A global network of optical atomic clocks will enable unprecedented measurement precision in fields including tests of fundamental physics, dark matter searches, geodesy, and navigation. Free-space laser links through the turbulent atmosphere are needed to fully exploit this global network, by enabling comparisons to airborne and spaceborne clocks. We demonstrate frequency transfer over a 2.4 km atmospheric link with turbulence comparable to that of a ground-to-space link, achieving a fractional frequency stability of 6.1×10^{-21} in 300 s of integration time. We also show that clock comparison between ground and low Earth orbit will be limited by the stability of the clocks themselves after only a few seconds of integration. This significantly advances the technologies needed to realize a global timescale network of optical atomic clocks.

DOI: 10.1103/PhysRevLett.128.020801

The establishment of a global network of optical atomic clocks will revolutionize fundamental physics experiments including tests of the general theory of relativity [1], investigations of the variability of fundamental constants [2], and searches for dark matter candidates, [3] among others [4–6]. Other scientific and technical applications such as geodesy [7,8], satellite navigation and timing [9], and radio astronomy [10] will also benefit from such a network. To implement this network on a global scale, free-space laser links will be necessary to link clocks where optical fiber links are not available.

To fully exploit the stability and precision of the atomic clocks, frequency transfer over the free-space laser links must have residual instabilities below that of the atomic clocks comprising the network. Optical atomic clocks are now reaching instabilities as low as 2×10^{-18} in 10 min [11], with future clocks expected to reach this level in an integration time as short as 100 s [12]. However, atmospheric turbulence induces both phase noise on the laser signal, which degrades the phase stability of the link, and amplitude noise, which degrades the signal-to-noise ratio, or causes complete dropouts of the link due to deep fades. Phase noise is caused by time-of-flight variations due to changes in the average refractive index of the atmosphere along the path of the laser, and this phase noise is much greater than on comparable lengths of optical fiber [13–15]. Higher order turbulence modes are responsible for amplitude noise of the laser signal by causing beam wander and scintillation [14,16]. Deep fades can occur tens to hundreds of times per second for ground-to-space links [13], limiting the integration time and, thus, ultimate transfer stability and precision of the timescale comparison.

Ultrastable frequency dissemination via optical fiber networks for optical atomic clock timescale comparison has been demonstrated over distances up to 1840 km [17–19]. Various groups [20–22] are now applying similar stabilization techniques to free-space laser links, where the amplitude noise caused by atmospheric turbulence imposes additional challenges. Notably, Ref. [23] recently demonstrated frequency comparison between optical atomic clocks over a 1.5 km horizontal free-space link with a residual instability of around one part in 10^{18}.

In this work, we demonstrate phase- and amplitude-stabilized free-space frequency transfer with a fractional frequency stability of 6.1×10^{-21} after only 300 s of integration, over a 2.4 km horizontal atmospheric link that was measured to have turbulence levels comparable to a link between ground and space [15,24]. From this result, and taking into account the reduced bandwidth due to the greater distances involved, we predict that a ground-to-space link based on the atmospheric stabilization technology demonstrated in this Letter will achieve a fractional frequency stability of around 1×10^{-20} within the viewing window of a low Earth orbit satellite transit. This means timescale comparisons via such a link will be limited by the stability of the clocks themselves after only a few seconds of integration. This achievement is a significant milestone in the development of ground-to-space laser links for optical atomic clock comparison through the turbulent atmosphere, and provides the technological

basis for the creation of a global timescale network of optical atomic clocks.

The free-space link was formed by transmitting an optical-frequency signal from an optical terminal located on the fifth floor of the University of Western Australia physics building (the local site), reflected off a corner-cube reflector (CCR) on a building 1.2 km away (the remote site), and received via the same optical terminal back at the local site. The terminal used first-order adaptive optics (a tip-tilt mirror) to suppress amplitude noise induced by the atmospheric turbulence and reduce the number of deep fades, while a separate fiberized phase-stabilization system was used to suppress phase noise. Figure 1 shows a schematic of the experimental setup.

The optical frequency transfer used a 1552 nm, narrow-band (<100 Hz) optical signal from an NKT Photonics X-15 fiber laser positioned at the local site transmitter. This "frequency transfer" signal was transmitted through the phase-stabilization system and then to the optical terminal. In the terminal, the optical signal passed through a fiber collimator, a 50:50 beam splitter, and into a ×15 Galilean beam expander (GBE) to produce a near-diffraction-limited laser beam with a waist of 34 mm (divergence 29 urad). The beam reflected off a 50 mm tip-tilt mirror and over the free-space link to the remote site, where it reflected off the 75 mm CCR and returned over the free-space link back to the optical terminal at the local site. The optical loss of the 2.4 km round-trip free-space link due to beam divergence and scattering was 11.2 dB.

Within the optical terminal, the returning beam reflected back off the tip-tilt mirror and through the GBE. The 50:50 splitter directed half of the optical power towards the fiber collimator, and the other half was focused onto a quadrant photodetector (QPD). The QPD produced X- and Y-position error signals, which fed a servo loop to control the two piezoactuators of the tip-tilt mirror. Closing the servo loop corrected fluctuations in the angle of arrival of the incoming beam, suppressing amplitude noise and reducing the number of deep fades. The terminal optics are aligned to ensure that centering the beam on the QPD also maintains the optimal alignment into the fiber collimator.

The power of the returning 1552 nm signal was below the minimum operating power of the QPD, so a second optical signal at 1555 nm from a Toptica DL 100 laser was combined with the signal from the phase stabilization system using a wavelength-division multiplexer (WDM) and delivered to the optical terminal. The higher power from this "beacon" laser was sufficient to operate the QPD after propagation over the 2.4 km link. The beacon light returning into the fiber was separated from the 1552 nm signal using the WDM, and directed to a photodetector to record the amplitude fluctuations over the link (Ampl.) on a dedicated 12 bit digitizer card at a sample rate of 20 kS/s.

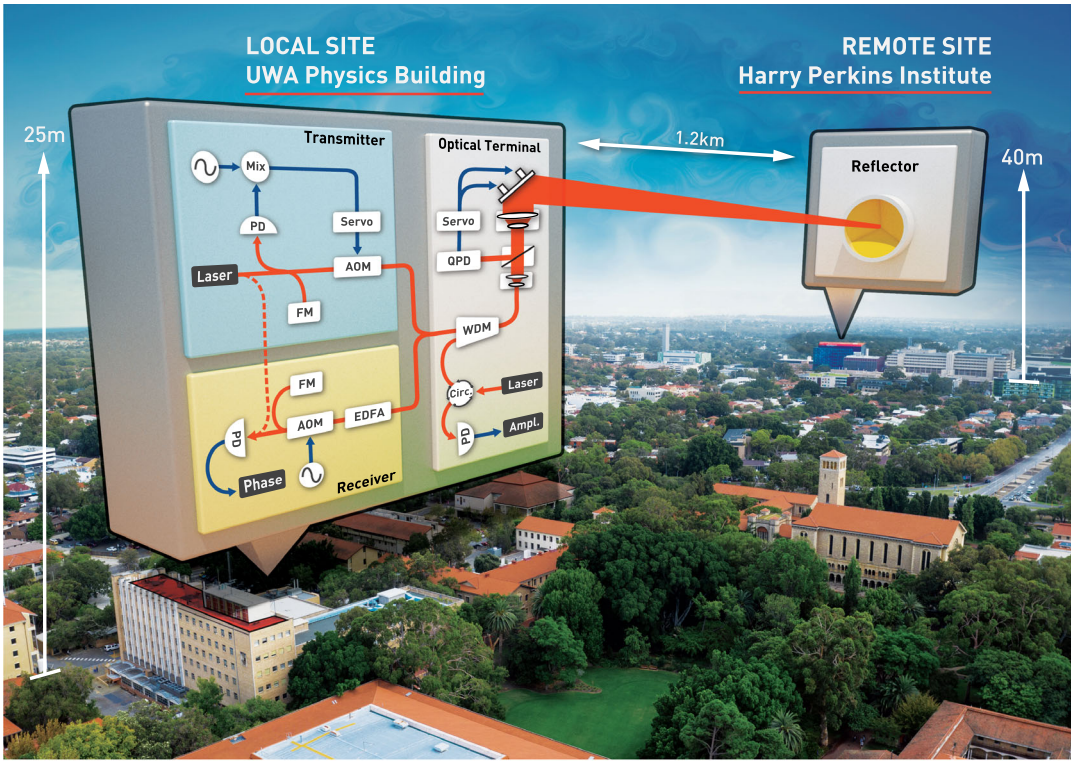

FIG. 1. Simplified schematic of the phase stabilization system integrated with the optical terminal. Blue lines, rf signals; and red lines, optical signals. Acronyms are defined in the text.

The phase stabilization of the optical frequency transfer was achieved using an imbalanced Michelson interferometer. At the transmitter, the frequency transfer signal was split using a fiberized 50:50 splitter. The main signal passed through an acousto-optic modulator (AOM) and was then delivered to the optical terminal and transmitted over the free-space link, where it picked up phase noise, before returning through the optical terminal and then to the receiver. In the receiver, the signal passed through a second AOM (for antireflection tagging). Part of the signal is reflected off a Faraday mirror, before completing the return journey along the same path back to the transmitter. A bidirectional erbium-doped fiber amplifier (EDFA) was placed at the input to the receiver to amplify the optical signal.

The returning signal is mixed (heterodyned) in the 50:50 splitter against a local copy of the frequency transfer signal that was reflected off a Faraday mirror in the short reference arm of the Michelson interferometer, and the resulting rf beat detected at a photodetector. This is then mixed down to dc using an rf local oscillator of frequency $2 \times (f_{\mathrm{AOM1}} + f_{\mathrm{AOM2}})$ to generate a phase error signal. The error signal is appropriately filtered in a phase-locked loop (PLL) that adjusts, via a voltage-controlled oscillator (Servo), the frequency of the transmitter AOM to compensate for the turbulence-induced phase noise.

The frequency transfer performance was measured by mixing the optical signal at the receiver with a reference signal split off from the frequency transfer laser. These data were recorded using a Microsemi 3120A phase noise test set and a Liquid Instruments Moku:Lab phasemeter. The 3120A is used to report the high-frequency performance of the system up to 100 kHz, while the Moku:Lab continuously recorded the phase at a sample rate of 1.95 kS/s and is used to report the long-term stability. Turbulence strength was measured using a camera-based scintillometer [24] that was constructed in-house based on the design presented in Ref. [25]. Weather data including wind speed and direction, temperature, and rainfall are also recorded.

Data acquisition runs were performed over two weeks in three configurations: (i) with amplitude stabilization (tip-tilt) on and phase stabilization off, (ii) amplitude stabilization off and phase stabilization on, and (iii) amplitude stabilization on and phase stabilization on. Runs were conducted for up to 24 h and stopped only to change configuration.

Figure 2 shows the fractional frequency stability of the free-space frequency transfer over the 2.4 km link expressed as modified Allan deviation (MDEV). With the phase stabilization system on, the MDEV averages down with integration time τ as $\tau^{-3/2}$, indicating the dominant noise source is white phase noise. This trend holds until thermal fluctuations begin to dominate the noise at integration times longer than a few tens of seconds. With the amplitude stabilization system off (blue), the best fractional frequency stability attained was 1×10^{-19} at an integration time of 60 s. With the amplitude stabilization system on (orange),

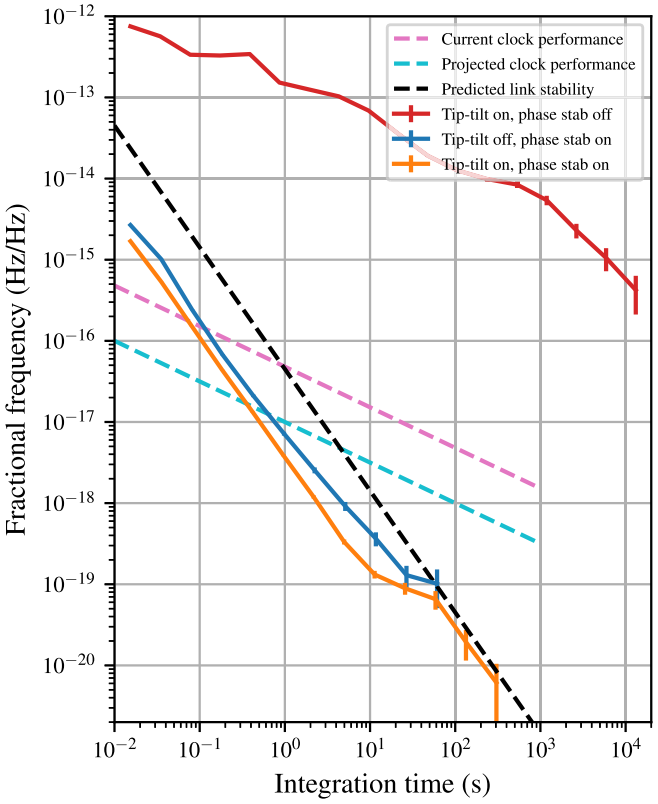

FIG. 2. Fractional frequency stability in terms of MDEV of the 2.4 km free-space link with amplitude stabilization (tip-tilt) on and phase stabilization off (red), amplitude stabilization off and phase stabilization on (blue), and amplitude stabilization on and phase stabilization on (orange). The dashed black line is the predicted stability for a ground-to-space link with phase stabilization bandwidth limited by the light round-trip time to a satellite 1000 km away. The dashed pink and dashed cyan lines represent current [11] and projected [12] optical clock performance.

the fractional frequency stability improves at all integration times (down to 7×10^{-20} at 60 s), as well as consistently allowing the phase synchronization to operate for significantly longer cycle-slip-free periods, reaching a best fractional frequency stability of 6.1×10^{-21} after 300 s. Over this link, the residual instability of the phase stabilization system is better than that of modern optical atomic clocks (dashed pink) [11] after less than 100 ms of integration. With phase stabilization off, the system attained a fractional frequency stability of 9.8×10^{-15} at 300 s. Additional fractional frequency results from other data runs are shown in Fig. S6 in the Supplemental Material [24].

Although the optics of the phase stabilization system were well insulated, fractional frequency performance at integration times longer than 10 s is limited by sensitivity of the system to thermal instabilities. Thermal instabilities result in mechanical changes in the length of out-of-loop fibers that produce false phase error signals, as well as noise within the phase measurement electronics (likely the internal PLLs).

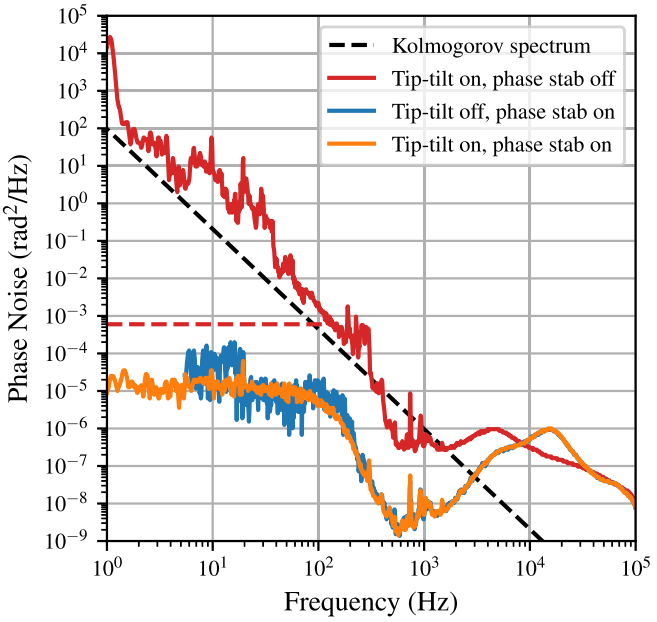

FIG. 3. Phase noise of the 2.4 km free-space link with amplitude stabilization (tip-tilt) on and phase stabilization off (red), amplitude stabilization off and phase stabilization on (blue), and amplitude stabilization on and phase stabilization on (orange). Dashed black line is the Kolmogorov spectrum for turbulence strength $C_n^2 = 5 \times 10^{-15}$ m$^{-2/3}$. Dashed red line is the compensated phase noise level achievable with a bandwidth of 150 Hz, which is the bandwidth limit imposed by the light round-trip time to a satellite 1000 km away.

The amplitude stabilization system significantly increased the robustness of the link and enabled regular cycle-slip-free operation for periods of around 30 min in low turbulence ($C_n^2 < 10^{-14}$ m$^{-2/3}$), with the longest cycle-slip free period being 104 min at an average turbulence strength of $C_n^2 = 6 \times 10^{-15}$ m$^{-2/3}$. For runs with the amplitude stabilization system off, the longest period between cycle slips was only 5 min. The measured turbulence strength for the traces in both Fig. 2 and Fig. 3 is $C_n^2 = 5 \times 10^{-15}$ m$^{-2/3}$.

Additional analysis of the performance of the amplitude stabilization system is shown in the Supplemental Material [24], including the measured cycle slip rate against different turbulence strengths (Fig. S4), and a comparison of the measured returned optical power against the expected returned optical power calculated from the measured turbulence strength (Fig. S5). The amplitude stabilization system significantly reduces the rate of cycle slips up to a turbulence strength of $C_n^2 = 1.5 \times 10^{-14}$ m$^{-2/3}$, corresponding to a Fried scale of 36 mm over the 2.4 km link, very close to the 34 mm fiber-coupled beam diameter of the optical terminal. This is consistent with previously reported results using similar optical terminals [16], and higher-order adaptive optics, or smaller apertures, will be required for the link to work in stronger turbulence.

Figure 3 shows the phase noise of the frequency transfer over the 2.4 km link corresponding to the measurements plotted in Fig. 2. With phase stabilization off, the phase noise at 1 Hz is 2×10^4 rad^2/Hz, which the phase stabilization system suppresses by nine orders of magnitude to 2×10^{-5} rad^2/Hz. The 3120A was unable to complete any measurement runs longer than around 20 s when the amplitude stabilization system was off (including at low turbulence) due to the large power drops caused by deep fades.

When the phase stabilization system is on, the phase noise is flat from 1 to 100 Hz before reducing at frequencies above 100 Hz. This broadband noise below 100 Hz is due to the EDFA reamplifying the already amplified signal returning from the folded link. As a result, the fractional frequency stabilities achieved in this experiment are currently limited by the broadband noise of the EDFA at integration times shorter than 10 s. This is unlikely to be a problem in a real, bistatic link, and this noise was not seen in point-to-point tests using the same EDFA and similar optical terminals [20].

The slope of the unstabilized phase noise (Fig. 3) is consistent with the theoretical value of $f^{-8/3}$ [26] up to a frequency of around 300 Hz, where phase noise of the frequency transfer laser begins to dominate the result, but is around 1 order of magnitude greater than predicted from the measured turbulence strength over the 2.4 km link assuming Kolmogorov turbulence [15].

Calculating the phase noise expected for a ground-to-space link to a spacecraft at an altitude of 500 km, approaching from 60° off the zenith, for the same ground-level turbulence strength, we find that the model from Ref. [15] predicts that the phase noise on such a ground-to-space link is very similar to the expected turbulence strength on a horizontal 2.4 km link. (Details of the calculation are provided in the Supplemental Material [24].) Therefore, the phase noise measured on the 2.4 km link during these trials is comparable to that expected on a link to low Earth orbit, so we can use this measured phase noise as a basis to estimate the performance of the phase stabilization system over a ground-to-space link.

For this ground-to-space link, the light round trip time limits the phase noise correction bandwidth to approximately 150 Hz (approximately 1000 km initial distance to the spacecraft). The dashed red line in Fig. 3 represents the level to which the atmospheric phase noise, solid red, could be stabilized with a bandwidth limit of 150 Hz. With this assumption, the results from Fig. 3 (backed up by Fig. S3 in Ref. [24]) are used to calculate a predicted fractional frequency stability that could be achieved for a ground-to-space link (Fig. 2, dashed black). Also shown in Fig. 2 are traces representing the stability of current (dashed pink) [11] and predicted (dashed cyan) [12] optical atomic clocks. This shows that the measurement precision of a ground-to-space clock comparison using this phase and

amplitude stabilization technology would be limited by the residual instabilities of the optical clocks after only a few seconds of integration. The laser link could achieve a fractional frequency stability of 1×10^{-20} after 300 s, a time period comparable to the viewing window of a satellite in low Earth orbit. This stability level is also consistent with the limits imposed by two-way differential phase noise caused by the point-ahead angle required to track the orbiting spacecraft [14,27].

This result shows that the phase and amplitude stabilization technologies presented in this Letter can provide the basis for ultraprecise timescale comparison of optical atomic clocks through the turbulent atmosphere. Future work will need to focus on tracking moving targets, which requires Doppler compensation. High-stability frequency-swept laser systems [28] are being developed to account for the large and rapidly changing Doppler shifts necessary to maintain an optical metrology link to a satellite in low Earth orbit. To support links with high attenuation, optical phase tracking has been achieved at levels of a few tens of femtowatts [29]. Applying these technologies to advanced optical ground stations currently under development [30] will enable the creation of a global optical atomic clock network for high-precision fundamental and applied science measurements. This technology also has promising applications in free-space laser communications [31] and quantum key distribution [32,33].

The authors would like to thank the Harry Perkins Institute of Medical Research for assistance in setting up the free-space link. This research is funded by the Australian Research Council's Centre of Excellence for Engineered Quantum Systems (EQUS, CE170100009) and the SmartSat Cooperative Research Centre (CRC. Research Project 1-01). D. R. G. is supported by a Forrest Research Foundation Fellowship. B. P. D-M. is supported by an Australian Government Research Training Program (RTP) Scholarship and a CRC Top-Up Scholarship.

D. R. G. and L. A. H. contributed equally to this work.

*david.gozzard@uwa.edu.au

[1] M. Takamoto, I. Ushijima, N. Ohmae, T. Yahagi, K. Kokado, H. Shinkai, and H. Katori, Test of general relativity by a pair of transportable optical lattice clocks, Nat. Photonics **14**, 411 (2020).

[2] R. M. Godun, P. B. R. Nisbet-Jones, J. M. Jones, S. A. King, L. A. M. Johnson, H. S. Margolis, K. Szymaniec, S. N. Lea, K. Bongs, and P. Gill, Frequency Ratio of Two Optical Clock Transitions in Yb + 171 and Constraints on the Time Variation of Fundamental Constants, Phys. Rev. Lett. **113**, 210801 (2014).

[3] A. Derevianko and M. Pospelov, Hunting for topological dark matter with atomic clocks, Nat. Phys. **10**, 933 (2014).

[4] P. Delva, A. Hees, and P. Wolf, Clocks in space for tests of fundamental physics, Space Sci. Rev. **212**, 1385 (2017).

[5] M. Takamoto, I. Ushijima, M. Das, N. Nemitz, T. Ohkubo, K. Yamanaka, N. Ohmae, T. Takano, T. Akatsuka, A. Yamaguchi, and H. Katori, Frequency ratios of Sr, Yb, and Hg based optical lattice clocks and their applications, C. R. Phys. **16**, 489 (2015).

[6] F. Riehle, Optical clock networks, Nat. Photonics **11**, 25 (2017).

[7] W. McGrew, X. Zhang, R. J. Fasano, S. A. Schäffer, K. Beloy, D. Nicolodi, R. C. Brown, N. Hinkley, G. Milani, M. Schioppo, and T. H. Yoon, Atomic clock performance enabling geodesy below the centimetre level, Nature (London) **564**, 87 (2018).

[8] B. P. Dix-Matthews, S. W. Schediwy, D. R. Gozzard, S. Driver, K. U. Schreiber, R. Carman, and M. Tobar, Methods for coherent optical Doppler orbitography, J. Geod. **94**, 1 (2020).

[9] W. Lewandowski and E. Arias, GNSS times and UTC, Metrologia **48**, S219 (2011).

[10] C. Clivati, R. Ambrosini, T. Artz, A. Bertarini, C. Bortolotti, M. Frittelli, F. Levi, A. Mura, G. Maccaferri, M. Nanni, and M. Negusini, A VLBI experiment using a remote atomic clock via a coherent fibre link, Sci. Rep. **7**, 40992 (2017).

[11] T. Bothwell, D. Kedar, E. Oelker, J. M. Robinson, S. L. Bromley, W. L. Tew, J. Ye, and C. J. Kennedy, JILA SrI optical lattice clock with uncertainty of 2.0×10^{-18}, Metrologia **56**, 065004 (2019).

[12] N. Hinkley, J. A. Sherman, N. B. Phillips, M. Schioppo, N. D. Lemke, K. Beloy, M. Pizzocaro, C. W. Oates, and A. D. Ludlow, An atomic clock with 10^{-18} instability, Science **341**, 1215 (2013).

[13] D. R. Gozzard, S. W. Schediwy, B. Stone, M. Messineo, and M. Tobar, Stabilized Free-Space Optical Frequency Transfer, Phys. Rev. Applied **10**, 024046 (2018).

[14] C. Robert, J. M. Conan, and P. Wolf, Impact of turbulence on high-precision ground-satellite frequency transfer with two-way coherent optical links, Phys. Rev. A **93**, 033860 (2016).

[15] L. C. Sinclair, F. R. Giorgetta, W. C. Swann, E. Baumann, I. Coddington, and N. R. Newbury, Optical phase noise from atmospheric fluctuations and its impact on optical time-frequency transfer, Phys. Rev. A **89**, 023805 (2014).

[16] W. C. Swann, L. C. Sinclair, I. Khader, H. Bergeron, J.-D. Deschênes, and N. R. Newbury, Low-loss reciprocal optical terminals for two-way time-frequency transfer, Appl. Opt. **56**, 9406 (2017).

[17] P. A. Williams, W. C. Swann, and N. R. Newbury, High-stability transfer of an optical frequency over long fiber-optic links, J. Opt. Soc. Am. B **25**, 1284 (2008).

[18] K. Predehl, G. Grosche, S. M. F. Raupach, S. Droste, O. Terra, J. Alnis, Th. Legero, T. W. Hänsch, T. Udem, R. Holzwarth, and H. Schnatz, A 920-kilometre optical fiber link for frequency metrology at the 19th decimal place, Science **336**, 441 (2012).

[19] S. Droste, F. Ozimek, Th. Udem, K. Predehl, T. W. Hänsch, H. Schnatz, G. Grosche, and R. Holzwarth, Optical-Frequency Transfer Over a Single-Span 1840 km Fiber Link, Phys. Rev. Lett. **111**, 110801 (2013).

[20] B. P. Dix-Matthews, S. W. Schediwy, D. R. Gozzard, E. Savalle, F-X. Esnault, T. Lévèque, C. Gravestock,

D. D'Mello, S. Karpathakis, M. Tobar, and P. Wolf, Point-to-point stabilized optical frequency transfer with active optics, Nat. Commun. **12**, 515 (2021).

[21] H. J. Kang, J. Yang, B. J. Chun, H. Jang, B. S. Kim, Y.-J. Kim, and S.-W. Kim, Free-space transfer of comb-rooted optical frequencies over an 18 km open-air link, Nat. Commun. **10**, 1 (2019).

[22] M. I. Bodine, J-D. Deschênes, I. H. Khader, W. C. Swann, H. Leopardi, K. Beloy, T. Bothwell, S. M. Brewer, S. L. Bromley, J. S. Chen, and S. A. Diddams, Optical atomic clock comparison through turbulent air, Phys. Rev. Research **2**, 033395 (2020).

[23] Boulder Atomic Clock Optical Network BACON Collaboration, Frequency ratio measurements at 18-digit accuracy using an optical clock network, Nature (London) **591**, 564 (2021).

[24] See Supplemental Material at http://link.aps.org/supplemental/10.1103/PhysRevLett.128.020801 for noise analysis and additional information.

[25] S. Manning, B. A. Clare, K. J. Grant, and K. A. Mudge, Development and implementation of a robust angle of arrival turbulence measurement system, Opt. Eng. **54**, 114104 (2015).

[26] J. M. Conan, G. Rousset, and P. Y. Madec, Wave-front temporal spectra in high-resolution imaging through turbulence, J. Opt. Soc. Am. A **12**, 1559 (1995).

[27] W. C. Swann, M. I. Bodine, I. Khader, J.-D. Deschênes, E. Baumann, L. C. Sinclair, and N. R. Newbury, Measurement of the impact of turbulence anisoplanatism on precision free-space optical time transfer, Phys. Rev. A **99**, 023855 (2019).

[28] N. Chiodo, K. Djerroud, O. Acef, A. Clairon, and P. Wolf, Lasers for coherent optical satellite links with large dynamics, Appl. Opt. **52**, 7342 (2013).

[29] S. P. Francis, T. T. Lam, K. McKenzie, A. J. Sutton, R. L. Ward, D. E. McClelland, and D. A. Shaddock, Weak-light phase tracking with a low cycle slip rate, Opt. Lett. **39**, 5251 (2014).

[30] F. Bennet, K. Ferguson, K. Grant, E. Kruzins, N. Rattenbury, and S. Schediwy, An Australian/New Zealand optical communications ground station network for next generation satellite communications, Proc. SPIE Free-Space Laser Commun. XXXII, 1127202 (2020).

[31] B. P. Dix-Matthews, D. R. Gozzard, S. F. E. Karpathakis, C. T. Gravestock, and S. W. Schediwy, Ultra-wideband free-space optical phase stabilization, IEEE Commun. Lett. **25**, 1610 (2021).

[32] C. Clivati *et al.*, Coherent phase transfer for real-world twin-field quantum key distribution, arXiv:2012.15199.

[33] M. Pittaluga, M. Minder, M. Lucamarini, M. Sanzaro, R. I. Woodward, M.-J. Li, Z. Yuan, and A. J. Shields, 600-km repeater-like quantum communications with dual-band stabilization, Nat. Photonics 15, 530 (2021).